Chapter 2
Flow and Functional Models for Rheological Properties of Fluid Foods

A flow model may be considered to be a mathematical equation that can describe rheological data, such as shear rate versus shear stress, in a basic shear diagram, and that provides a convenient and concise manner of describing the data. Occasionally, such as for the viscosity versus temperature data during starch gelatinization, more than one equation may be necessary to describe the rheological data. In addition to mathematical convenience, it is important to quantify how magnitudes of model parameters are affected by state variables, such as temperature, and the effect of structure/composition (e.g., concentration of solids) of foods and establish widely applicable relationships that may be called functional models.

Rheological models may be grouped under the categories: (1) empirical, (2) theoretical, and (3) structural. Obviously, an empirical model, such as the power law (Eq. 2.3), is deduced from examination of experimental data. A theoretical model is derived from fundamental concepts and it provides valuable guidelines on understanding the role of structure. It indicates the factors that influence a rheological parameter. The Krieger–Dougherty model (Krieger 1985) (Eq. 2.26) for relative viscosity is one such model. Another theoretical model is that of Shih et al. (1990) that relates the modulus to the fractal dimension of a gel.

A structural model is derived from considerations of the structure and often kinetics of changes in it. It may be used, together with experimental data, to estimate values of parameters that help characterize the rheological behavior of a food sample. One such model is that of Casson (Eq. 2.6) that has been used extensively to characterize the characteristics of foods that exhibit yield stress. Another structural model is that of Cross (1965) (Eq. 2.14) that has been used to characterize flow behavior of polymer dispersions and other shear-thinning fluids. While application of structure-based models to rheological data provides useful information, structure-based analysis can provide valuable insight in to the role of the structure of a dispersed system. For example, as discussed in Chap. 5, it allows for estimating the contributions of interparticle bonding and network of particles of dispersed systems.

Flow models have been used also to derive expressions for velocity profiles and volumetric flow rates in tube and channel flows, and in the analysis of heat transfer phenomenon. Numerous flow models can be encountered in the rheology literature

M. A. Rao, *Rheology of Fluid, Semisolid, and Solid Foods,* Food Engineering Series,
DOI 10.1007/978-1-4614-9230-6_2,

Table 2.1 Some two- and three-parameter flow models for describing shear rate ($\dot{\gamma}$) versus shear stress (σ) data

$\sigma = \eta\dot{\gamma}$	Newtonian model*
$\sigma = \dfrac{\dot{\gamma}}{\left[\dfrac{1}{\eta_0} + K_{\mathrm{E}}\left(\sigma\right)^{(1/n_{\mathrm{E}})-1}\right]}$	Ellis model for low-shear rate data containing η_0 (Brodkey 1967)
$\sigma = \left[\eta_\infty\dot{\gamma} + K_{\mathrm{s}}\dot{\gamma}^{n_{\mathrm{s}}}\right]$	Sisko model for high-shear rate data containing η_∞ (Brodkey 1967)
$\eta_{\mathrm{a}} = \eta_\infty + \dfrac{\eta_0 - \eta_\infty}{1 + (\alpha_{\mathrm{c}}\dot{\gamma})^m}$	Cross model for data over a wide range of shear rates*
$\eta_{\mathrm{a}} = \eta_\infty + \dfrac{\eta_0 - \eta_\infty}{[1 + (\lambda_{\mathrm{c}}\dot{\gamma})^2]^N}$	Carreau model for data over a wide range of shear rates*
$\sigma = \mathrm{K}\,\dot{\gamma}^n$	Power law model used extensively in handling applications*
$\sigma - \sigma_0 = \eta'\dot{\gamma}$	Bingham model*
$\sigma - \sigma_{0\mathrm{H}} = K_K\dot{\gamma}^{n_{\mathrm{H}}}$	Herschel–Bulkley model*
$\sigma^{0.5} = K_{0\mathrm{c}} + K_{\mathrm{c}}(\dot{\gamma})^{0.5}$	Casson model used especially in treating data on chocolates*
$\sigma^{0.5} - \sigma_{0\mathrm{M}} = K_{\mathrm{M}}\dot{\gamma}^{n_{\mathrm{M}}}$	Mizrahi and Berk (1972) model is a modification of the Casson model
$\sigma^{n_1} = \sigma_0^{n_1} + \eta_\infty(\dot{\gamma})^{n_2}$	Generalized model of Ofoli et al. (1987)*
$\sigma = [(\sigma_{o\mathrm{V}})^{1/n_{\mathrm{V}}} + K_{\mathrm{V}\dot{\gamma}}]^{n_{\mathrm{V}}}$	Vocadlo (Vocadlo and Moo Young 1969) model

*Discussed in text

and some from the food rheology literature are listed in Table 2.1. Also, here those models that have found extensive use in the analysis of the flow behavior of fluid foods are discussed. Models that account for yield stress are known as viscoplastic models (Bird et al. 1982). For convenience, the flow models can be divided in to those for time-independent and for time-dependent flow behavior.

Time-Independent Flow Behavior

Newtonian Model

The model for a Newtonian fluid is described by the equation:

$$\sigma = \eta\gamma \tag{2.1}$$

As per the definition of a Newtonian fluid, the shear stress, σ, and the shear rate, $\dot{\gamma}$, are proportional to each other, and a single parameter, η, the viscosity, characterizes the data. For a Bingham plastic fluid that exhibits a yield stress, σ_0, the model is:

$$\sigma - \sigma_0 = \eta'\gamma \tag{2.2}$$

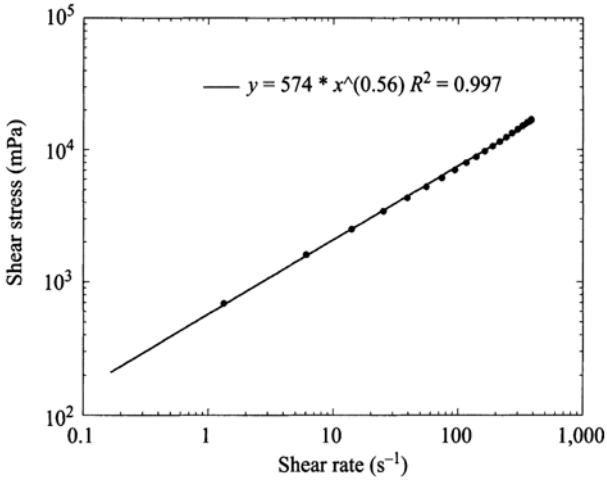

Fig. 2.1 Plot of log shear rate ($\dot{\gamma}$) versus log shear stress (σ) for a 2.6% Tapioca starch dispersion heated at 67 °C for 5 min (Tattiyakul 1997) to illustrate applicability of the power law model

where, η' is called the Bingham plastic viscosity.

As shown in Fig. 2.1, the Newtonian model and the Bingham plastic model can be described by straight lines in terms of shear rate and shear stress, and the former can be described by one parameter η and the latter by two parameters: η' and σ_0, respectively. However, the shear rate–shear stress data of shear-thinning and shear-thickening fluids are curves that require more than one parameter to describe their data. Given that the equation of a straight line is simple, it is easy to understand attempts to transform shear rate–shear stress data in to such lines. An additional advantage of a straight line is that it can be described by just two parameters: the slope and the intercept.

Power Law Model

Shear stress–shear rate plots of many fluids become linear when plotted on double logarithmic coordinates and the power law model describes the data of shear-thinning and shear thickening fluids:

$$\sigma = K\dot{\gamma}^n \tag{2.3}$$

where, K the consistency coefficient with the units: Pa s^n is the shear stress at a shear rate of 1.0 s^{-1} and the exponent n, the flow behavior index, is dimensionless that reflects the closeness to Newtonian flow. The parameter K is sometimes referred to as consistency index. For the special case of a Newtonian fluid ($n = 1$), the consistency index K is identically equal to the viscosity of the fluid, η. When the magnitude of $n < 1$ the fluid is shear-thinning and when $n > 1$ the fluid is shear-thickening in nature. Taking logarithms of both sides of Eq. 2.3:

$$\log\sigma = \log K + n\log\dot{\gamma} \tag{2.4}$$

The parameters K and n are determined from a plot of log σ versus log $\dot{\gamma}$, and the resulting straight line's intercept is log K and the slope is n. If a large number of σ versus $\dot{\gamma}$ data points, for example, >15 (it is easy to obtain large number of points with automated viscometers) are available, linear regression of log $\dot{\gamma}$ versus log σ will provide statistically best values of K and n. Nevertheless, a plot of experimental and predicted values of log $\dot{\gamma}$ and log σ is useful for observing trends in data and ability of the model to follow the data. Figure 2.1 illustrates applicability of the power law model to a 2.6% tapioca starch dispersion heated at 67 °C for 5 min. Linear regression techniques also can be used for determination of the parameters of the Herschel–Bulkley (when the magnitude of the yield stress is known) and the Casson models discussed later in this chapter.

Because it contains only two parameters (K and n) that can describe shear rate–shear stress data, the power law model has been used extensively to characterize fluid foods. It is also the most used model in studies on handling of foods and heating/cooling of foods. Extensive compilations of the magnitudes of power law parameters can be found in Holdsworth (1971, 1993). Because it is convenient to group foods in to commodities, a compilation of magnitudes of power law parameters of several food commodities are given in Chap. 5. In addition, the influence of temperature in quantitative terms of activation energies, and the effect of concentration of soluble and insoluble solids on the consistency index are given.

Although the power law model is popular and useful, its empirical nature should be noted. One reason for its popularity appears to be due to its applicability over the shear rate range: $10^1 - 10^4$ s^{-1} that can be obtained with many commercial viscometers. Often, the magnitudes of the consistency and the flow behavior indexes of a food sample depend on the specific shear rate range being used so that when comparing the properties of different samples an attempt should be made to determine them over a specific range of shear rates. One drawback of the power law model is that it does not describe the low-shear and high-shear rate constant-viscosity data of shear-thinning foods.

Herschel–Bulkley Model

When yield stress of a food is measurable, it can be included in the power law model and the model is known as the Herschel–Bulkley model:

$$\sigma - \sigma_{0H} = K_{H\dot{\gamma}^{nH}} \tag{2.5}$$

where, $\dot{\gamma}$ is shear rate (s^{-1}), σ is shear stress (Pa), n_H is the flow behavior index, K_H is the consistency index, and σ_{0H} is yield stress. It is noted here that the concept of yield stress has been challenged (Barnes and Walters 1989) because a fluid may deform minutely at stress values lower than the yield stress. Nevertheless, yield stress may be considered to be an engineering reality and plays an important role in many food products.

If the yield stress of a sample is known from an independent experiment, K_H and n_H can be determined from linear regression of log σ—σ_{0H} versus log($\dot{\gamma}$) as

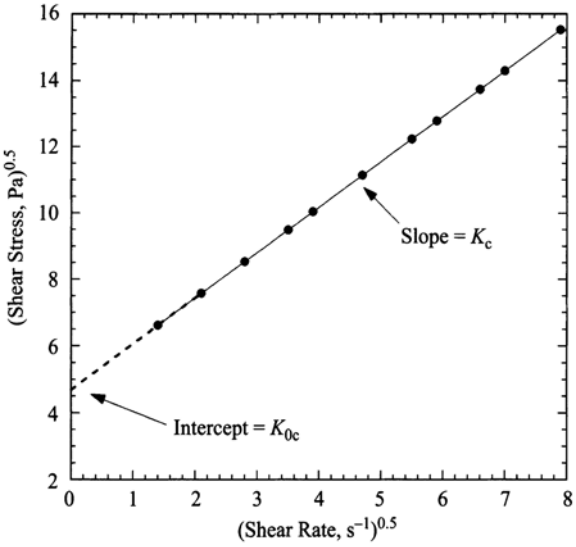

Fig. 2.2 Plot of $(\dot{\gamma})^{0.5}$ versus $(\sigma)^{0.5}$ for a food that follows the Casson model. The square of the intercept is the yield stress and that of slope is the Casson plastic viscosity

the intercept and slope, respectively. Alternatively, nonlinear regression technique was used to estimate σ_{0H}, K_H, and n_H (Rao and Cooley 1983). However, estimated values of yield stress and other rheological parameters should be used only when experimentally determined values are not available. In addition, unless values of the parameters are constrained a priori, nonlinear regression provides values that are the best in a least squares sense and may not reflect the true nature of the test sample.

Casson Model

The Casson model (Eq. 2.6) is a structure-based model (Casson 1959) that, although was developed for characterizing printing inks originally, has been used to characterize a number of food dispersions:

$$\sigma^{0.5} = K_{0c} + K_c(\dot{\gamma})^{0.5} \tag{2.6}$$

For a food whose flow behavior follows the Casson model, a straight line results when the square root of shear rate, $(\dot{\gamma})^{0.5}$, is plotted against the square root of shear stress, $(\sigma)^{0.5}$, with slope K_c and intercept K_{0c} (Fig. 2.2). The Casson yield stress is calculated as the square of the intercept, $\sigma_{0c} = (K_{0c})^2$ and the Casson plastic viscosity as the square of the slope, $\eta_{ca} = (K_c)^2$. The data in Fig. 2.2 are of Steiner (1958) on a chocolate sample. The International Office of Cocoa and Chocolate has adopted the Casson model as the official method for interpretation of flow data on chocolates. However, it was suggested that the vane yield stress would be a more reliable measure of the yield stress of chocolate and cocoa products (Servais et al. 2004).

The Casson plastic viscosity can be used as the infinite shear viscosity, η_∞, (Metz et al. 1979) of dispersions by considering the limiting viscosity at infinite shear rate:

$$\left(\frac{d\sigma}{d\dot{\gamma}}\right)_{\dot{\gamma}\to\infty} = \left(\frac{d(\sqrt{\sigma})}{d\dot{\gamma}}\frac{d\sigma}{d(\sqrt{\sigma})}\right)_{\dot{\gamma}\to\infty} \tag{2.7}$$

Using the Casson equation the two terms in the right-hand side bracket can be written as:

$$\frac{d(\sqrt{\sigma})}{d\dot{\gamma}} = \frac{K_C}{2\sqrt{\dot{\gamma}}} \tag{2.8}$$

and

$$\frac{d\sigma}{d(\sqrt{\sigma})} = 2\sqrt{\sigma} \tag{2.9}$$

Combining the above two equations,

$$\eta_\infty = \eta_{Ca} = (K_C)^2 \tag{2.10}$$

Quemada Model

Quemada et al. (1985) proposed a viscosity equation for dispersed systems based on zero-shear, η_0, and infinite-shear, η_∞, viscosities, and a structural parameter, λ, dependent on the shear rate, that may be written as:

$$\frac{\eta}{\eta_\infty} = \frac{1}{\left\{1-\left[1-\left(\frac{\eta_\infty}{\eta_0}\right)^{0.5}\right]\lambda\right\}^2} \tag{2.11}$$

where,

$$\lambda = \frac{1}{\left[1+(t_C\dot{\gamma})^{0.5}\right]} \tag{2.12}$$

The time constant t_c is related to the rate of aggregation of particles due to Brownian motion. For highly concentrated dispersed systems, η_∞ will be much lower than η_0, so that $(\eta_\infty/\eta_0)<<1$ and the dispersion may have a yield stress, and Eq. (2.11) reduces to the Casson model (Eq. 2.6) (Tiu et al. 1992) with the Casson yield stress, $\sigma_{0c}=(\eta_\infty/t_c)$. Thus the Casson–Quemada models can be used to examine dispersions whose rheological behaviors range from only shear-thinning to shear thinning with yield stress. The Casson–Quemada models were used to study the role of cocoa sol-

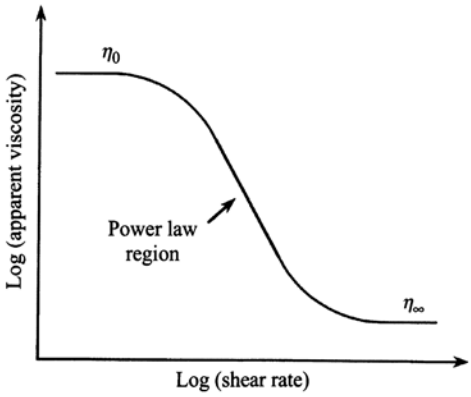

Fig. 2.3 Plot of shear rate versus apparent viscosity for shear thinning foods identifying three separate regions: a zero-shear viscosity at low shear rates, a power law region at intermediate shear rates, and an infinite-shear viscosity at high-shear rates. Often, only data in the power law region are obtained

ids and cocoa butter on cocoa dispersions (Fang et al. 1996, 1997) to be discussed in Chap. 5.

A general model for shear rate–shear stress data that under specific assumptions reduces to the Herschel–Bulkley, the Casson, and other models was presented by Ofoli et al. (1987):

$$\sigma^{n_1} = \sigma_0^{n_1} + \eta_\infty (\dot{\gamma})^{n_2} \tag{2.13}$$

where, n_1 and n_2 are constants, and η_∞ is the infinite shear viscosity. It is important to note that one model may be applicable at low-shear rates and another at high-shear rates (Dervisoglu and Kokini 1986). While applicability of the flow models themselves may be interesting, it is much more important to study the role of food composition on a model's parameters and apply the model to better understand the nature of foods.

Apparent Viscosity—Shear Rate Relationships of Shear-Thinning Foods

At sufficiently high polymer concentrations, most shear-thinning biopolymer (also called a gum or a hydrocolloid) dispersions exhibit similar three-stage viscous response when sheared over a wide shear rate range (Fig. 2.3): (1) at low-shear rates, they show Newtonian properties with a constant zero-shear viscosity (η_0) over a limited shear range that is followed by, (2) a shear-thinning range where solution viscosity decreases in accordance with the power law relationship; the reciprocal of the shear rate at which the transition from Newtonian to pseudoplastic behavior occurs is the characteristic time or the time constant, and (3) attains a limiting and constant infinite-shear-viscosity (η_∞). The three regions may be thought of being

due rearrangement in the conformation of the biopolymer molecules in the dispersion due to shearing. In stage 1 when the magnitude of $\dot{\gamma}$ is low, there is little rearrangement of the polymer chains, while in stage 2 the chains undergo gradual rearrangement with $\dot{\gamma}$ resulting in a power law behavior. In stage 3, the shear rate is sufficiently high that the polymer chains do not undergo much rearrangement.

Cross and Carreau Models

The apparent viscosity (η_a) of the solution can be correlated with shear rate ($\dot{\gamma}$) using the Cross (Eq. 2.14) or the Carreau (Eq. 2.15) equations, respectively.

$$\eta_a = \eta_\infty + \frac{\eta_0 - \eta_\infty}{1 + (\alpha_c \gamma)^m} \tag{2.14}$$

$$\eta_a = \eta_\infty + \frac{\eta_0 - \eta_\infty}{[1 + (\lambda_c \dot{\gamma})^2]^N} \tag{2.15}$$

where, α_c and λ_c are time constants related to the relaxation times of the polymer in solution and m and N are dimensionless exponents. Because magnitudes of $\eta\infty$ of food polymer dispersions with concentrations of practical interest are usually very low in magnitude, they are difficult to determine experimentally. Therefore, to avoid consequent errors in estimation of the other rheological parameters in Eqs. 2.14 and 2.15, often η_∞ has been neglected (Abdel-Khalik et al. 1974; Lopes da Silva et al. 1992). The Cross and Carreau models described well the shear dependence of aqueous dispersions of high methoxyl pectins and locust bean gum (Lopes da Silva et al. 1992), konjac flour gum (Jacon et al. 1993), and mesquite gum solution (Yoo et al. 1995), and other gums (Launay et al. 1986). In general, the model of Cross has been used in studies in Europe and that of Carreau in North America. In Chap. 4, the applicability of the Cross and Carreau models to locust bean gum dispersions will be discussed in more detail.

For small values of η_∞, the Cross exponent m tends to a value $(1-n)$, where n is the power law flow behavior index (Launay et al. 1986; Giboreau et al. 1994). For the shear rate, $\dot{\gamma}_c$ where $\eta_{ap}=(\eta_0+\eta_\infty)/2$, the Cross time constant $\alpha_c = 1/\dot{\gamma}_c$. Generally, $\dot{\gamma}_c$ gives an order of magnitude of the critical shear rate marking the end of the zero shear rate Newtonian plateau or the onset of the shear-thinning region. It is therefore important to recognize the shear rate dependence of the rheological behavior of polysaccharide polymers in solution and the difficulty involved in obtaining experimental data over the applicable shear rate range of $10^{-6}-10^4$ s^{-1} (Barnes et al. 1989). The low-shear rate region of about $10^{-3}-10^0$ is often used for the characterization and differentiation of structures in polysaccharide systems through the use of stress controlled creep and non destructive oscillatory tests. The shear rate range of about 10^1-10^4 s^{-1} falls within the operational domain of most commercial

rheometers, so that the range of $10^{-3} - 10^{4}$ s^{-1} can sometimes be effectively covered by a combination of measuring procedures and instruments.

Both the Carreau and the Cross models can be modified to include a term due to yield stress. For example, the Carreau model with a yield term given in Eq. (2.16) was employed in the study of the rheological behavior of glass-filled polymers (Poslinski et al. 1988):

$$\eta_a = \sigma_0 \dot{\gamma}^{-1} + \eta_p \left[1 + (\lambda_p \dot{\gamma})^2\right]^{-N} \tag{2.16}$$

where, σ_0 is the yield stress, η_p is the plateau viscosity, and λ_p and N are constants to be determined from experimental data. Rayment et al. (1998) interpreted the rheological behavior of guar gum dispersions containing raw rice starch in terms of the Cross model with yield stress (Eq. 2.17). We note that, when yield stress is exhibited, the term plateau viscosity is used instead of zero-shear viscosity:

$$\eta_a = \sigma_0 \dot{\gamma}^{-1} + \eta_P \left[1 + (\alpha_c \dot{\gamma})\right]^{-m} \tag{2.17}$$

Models for Time-Dependent Flow Behavior

Considerable care should be exercised in determining reliable time-dependent rheological data because of the often unavoidable modification in structure due to sample handling and during loading the sample in a viscometer or rheometer measuring geometry. Nevertheless, with careful attention to details, such as allowing a sample to relax in the rheometer measuring geometry, rheological data can be obtained to characterize time-dependent rheological behavior.

Weltman Model

The Weltman (1943) model has been used to characterize thixotropic (Paredes et al. 1988) behavior and of antithixotropic behavior (da Silva et al. 1997) of foods:

$$\sigma = A - B \log t \tag{2.18}$$

where, σ is shear stress (Pa), t is time (s), and A (value of stress at $t = 1$ s) and B are constants. A plot of σ versus log time should result in a straight line. In thixotropic behavior B takes negative values and in antithixotropic behavior it takes positive values. Table 2.2 shows typical magnitudes of the constants A and B for cross-linked waxy maize starch dispersions.

Table 2.2 Weltman Equation parameters for cross-linked waxy maize gelatinized starch dispersions. (Da Silva et al. 1997)

		Shear rate (s^{-1})			
Weltman Parameter	Conc. (%)	50	100	200	300
A	3	6.97×10^{-2}	5.76×10^{-2}	4.22×10^{-2}	
	4	2.97×10^{-1}	2.08×10^{-1}	1.72×10^{-1}	9.54×10^{-2}
	5		5.39×10^{-1}	3.88×10^{-1}	3.55×10^{-1}
B	3	1.58×10^{-3}	5.71×10^{-4}	1.66×10^{-5}	
	4	3.15×10^{-3}	2.07×10^{-3}	5.29×10^{-3}	7.83×10^{-3}
	5		8.30×10^{-5}	1.06×10^{-2}	8.79×10^{-3}
Correlation coef.	3	1.00	1.00	1.00	
	4	1.00	1.00	1.00	1.00
	5		1.00	1.00	1.00

Tiu–Boger Model

A model to study thixotropic behavior of foods exhibiting yield stress was devised by Tiu and Boger (1974) who studied the time-dependent rheological behavior of mayonnaise by means of a modified Herschel–Bulkley model:

$$\sigma = \lambda\left[\sigma_{0\mathrm{H}} + K_{\mathrm{H}}\left(\dot{\gamma}\right)^{n\mathrm{H}}\right] \tag{2.19}$$

where, σ is the shear stress (Pa), $\dot{\gamma}$ is the shear rate (s^{-1}), λ is a time-dependent structural parameter that ranges from an initial value of unity to an equilibrium value λ_e, σ_{0H} is the yield stress (Pa), K_H is the consistency index (Pa s^n), and n_H is the flow behavior index. The decay of the structural parameter with time was assumed to obey a second-order equation:

$$\frac{\mathrm{d}\lambda}{\mathrm{d}t} = -k_1(\lambda - \lambda_{\mathrm{e}})^2 \tag{2.20}$$

where, the constant k_1 is a function of shear rate to be determined experimentally. While the determination of σ_{0H}, and n_H is straight forward, estimation of k_1 and λ_e requires the use of values of apparent viscosities (η_a) (Tiu and Boger 1974):

$$\lambda = \frac{\eta_{\mathrm{a}}\dot{\gamma}}{\sigma_{0\mathrm{H}} + K_{\mathrm{H}}\dot{\gamma}^{n\mathrm{H}}} \tag{2.21}$$

and

$$\frac{\mathrm{d}\eta_{\mathrm{a}}}{\mathrm{d}t} = -a_1\left(\eta_{\mathrm{a}} - \eta_{\mathrm{e}}\right)^2 \tag{2.22}$$

where,

$$a_1(\dot{\gamma}) = \frac{k_1 \dot{\gamma}}{\sigma_{0H} + K_H \dot{\gamma}^{nH}} \tag{2.23}$$

It can be shown (Tiu and Boger 1974), that a plot of $1/(\eta_a — \eta_e)$ versus time will yield a straight line of slope a_1 and repeating the procedure at other shear rates will establish the relationship between a_1 and $\dot{\gamma}$, and hence k_1 and $\dot{\gamma}$ from Eq. 2.20. For a commercial mayonnaise sample, values of the different parameters were: $\lambda_e = 0.63$, $\sigma_{0H} = 7.0$ Pa, $K_H = 28.5$ Pa s^n, $n_H = 0.32$, and k_1 was a weak function of shear rate; specifically, $k_1 = 0.012\ \dot{\gamma}^{0.13}$ (Tiu and Boger 1974).

Role of Solids Fraction in Rheology of Dispersions

Following Einstein's work (Einstein 1906, 1911) (Eq. 2.24) on dilute rigid sphere dispersions, models for estimating viscosity of concentrated nonfood dispersions of solids are based on volume fraction (ϕ) of the suspended granules and the relative viscosity of the dispersion, $\eta_r = (\eta/\eta_s)$, where η is the viscosity of the dispersion η_s is the viscosity of the continuous phase (Jinescu 1974; Metzner 1985).

$$\eta_r = 1 + 2.5\,\phi \tag{2.24}$$

Metzner (1985) pointed out that at high solids concentration levels, the theoretical equation (Eq. 2.25) of Frankel and Acrivos appears to do a good job of portraying experimental data of rigid solids dispersed in polymer melts.

$$\eta_r = \frac{9}{8}\left[\frac{(\phi/\phi_m)^{1/3}}{1 - (\phi/\phi_m)^{1/3}}\right] \tag{2.25}$$

Wildemuth and Williams (1984) modeled the η_r of rigid sphere suspensions with a shear-dependent maximum volume fraction (ϕ_m). The applicability of a shear dependent ϕ_m (Wildemuth and Williams 1984) to food dispersions has not been tested.

The Krieger–Dougherty (1959) relationship (Eq. 2.26) is based on the assumption that an equilibrium exists between individual spherical particles and dumbbells that continuously form and dissociate:

$$\eta_r = \left(1 - \frac{\phi}{\phi_m}\right)^{-[\eta]\phi_m} \tag{2.26}$$

where, $[\eta]$ and ϕ_m are the intrinsic viscosity and maximum packing fraction of solids. Theoretically, $[\eta]$ should be 2.5 for rigid spheres and ϕ_m should be about 0.62 if the spheres are of uniform diameter (Krieger 1985), but Choi and Krieger (1986) found it necessary to use values of $[\eta]$ of 2.65–3.19 to fit Eq. 2.25 to viscosity-

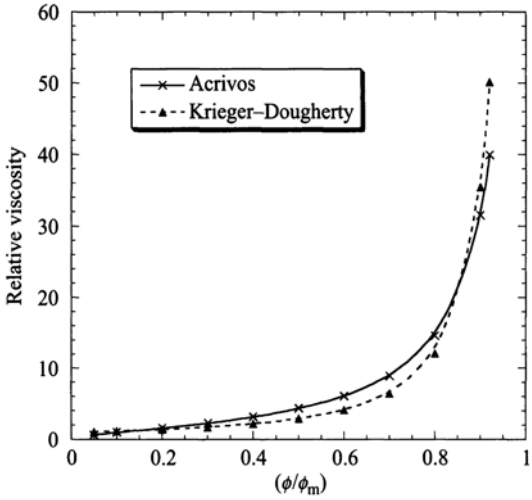

Fig. 2.4 Relative viscosity versus volume fraction ratio ($\varnothing/\varnothing_m$) predicted by models of Frankel–Acrivos and Krieger–Dougherty $\varnothing_m = 0.62$ and $[\eta] = 2.5$

volume fraction data on sterically stabilized poly methylmethacrylate spheres. For calculating values of % according to the Krieger–Dougherty equation, a value of $\phi_m = 0.62$ was assumed (Choi and Krieger 1986). Both Eqs. 2.24 and 2.25 contain the ratio of volume fraction of solids in a dispersion to the maximum volume fraction and the values of η_r predicted (Fig. 2.4) are close to each other. In Fig. 2.4 for the Krieger–Dougherty model, ϕ_m was taken to be 0.62 and $[\eta]$ to be 2.5. It is emphasized that the above equations were derived for rigid solids; because of the polydisperse and deformable nature of gelatinized starch dispersions, it is not surprising that attempts to predict their viscosity with Eq. 2.25 (Noel et al. 1993; Ellis et al. 1989) were not successful.

Most food particles are not spherical in shape so that the empirical equation (Eq. 2.25) that described well (Kitano et al. 1981; Metzner 1985) the relative viscosity versus concentration behavior of suspensions of spheres and fibers with aspect (L/D) ratios ≤30 in polymer melts is of interest:

$$\eta_r = [1 - (\phi/A)]^{-2} \tag{2.27}$$

Equation 2.27 is an empirical equation that is a simple modification of the Maron–Pierce equation for dispersions of spherical rigid solids:

$$\eta_r = [1 - (\phi/\phi_m)]^{-2} \tag{2.28}$$

For fluids that obey the power law model (Eq. 2.3), Metzner (1985) suggested that the viscosities of the suspension and of the continuous phase be evaluated at the same shearing stress. For rigid particles, the value of A decreases as aspect ratio of suspended particles increases; for example, when the aspect ratio is 1.0 (smooth sphere) the magnitude of A is 0.68, and when the aspect ratio is 6–8 (rough crystal)

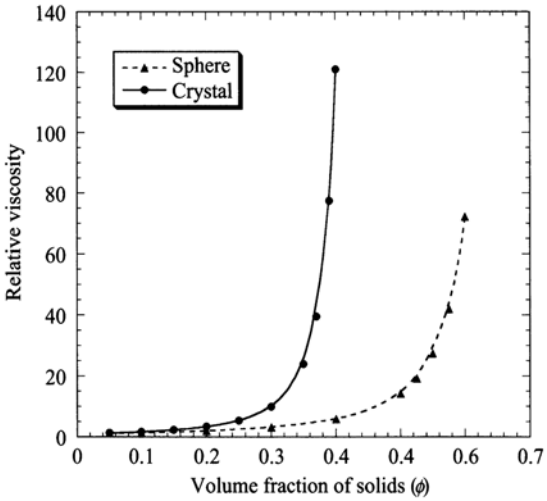

Fig. 2.5 Relative viscosity, η_r, versus volume fraction of solids predicted by model of Kitano et al. (1981) for rigid spheres ($A=0.68$) and crystal-like solids ($A=0.44$)

A is 0.44 (Metzner 1985). The shape of many food particles is not spherical and may be considered to be closer to a rough crystal. Figure 2.5 illustrates predictions of η_r by Eq. 2.25 for dispersions of spherical and rough crystal-like rigid particles. For the dispersion of rough crystal-like rigid particles, high values of η_r are attained at solids loading much lower than for rigid spherical particles (Fig. 2.5).

Because of the compressible nature of food dispersions, the direct determination of the magnitude of ϕ is not easy as it depends on the centrifugal force employed in the separation of the phases. Therefore, rheological properties of plant food dispersions, such tomato concentrate and concentrated orange juice, are based on the mass of pulp. In starch dispersions, they are based on the mass fraction of starch granules, denoted as cQ, as described in Chap. 4.

Applicability of Eq (2.27) for suspensions of tomato pulp of narrow size distribution was shown by Yoo and Rao (1994). Tomato pulp particles with average particle diameters 0.71 and 0.34 mm retained on the two sieves (sieve no. 40 and 60, respectively) were produced (Fig. 2.6). The apparent average diameters were calculated as in Kimball and Kertesz (1952). Because the Casson viscosity was shown to be equal to infinite shear viscosity (Metz et al. 1979), it is less arbitrary and has a theoretical foundation. Considering the values of the single parameter A of tomato puree samples (Fig. 2.7), the particle shape appears to be close to rough or irregular spherical shape (Yoo and Rao 1994). Also, the magnitude of A of the TP6 sample was higher than that of the TP4 sample because of its lower aspect ratio.

Quemada et al. (1985) proposed a model similar to that given by Eq. 2.27, but with $A=0.5$ and the structural parameter $k=1.80$:

$$\eta_r = \left(1 - \frac{1}{2}k\phi\right)^{-2} \tag{2.29}$$

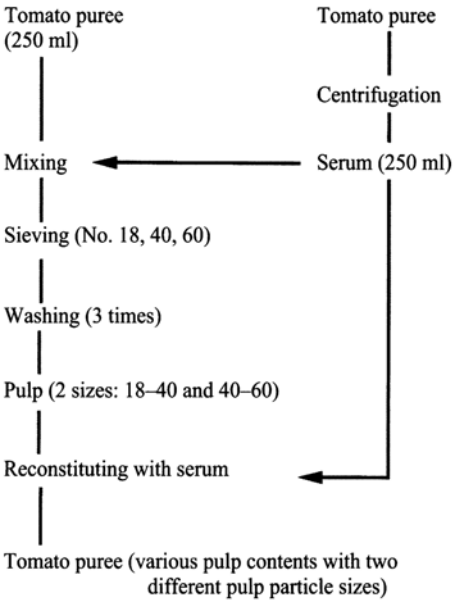

Fig. 2.6 Procedure for producing tomato pulp particles of narrow particle size distribution. (Yoo and Rao 1994)

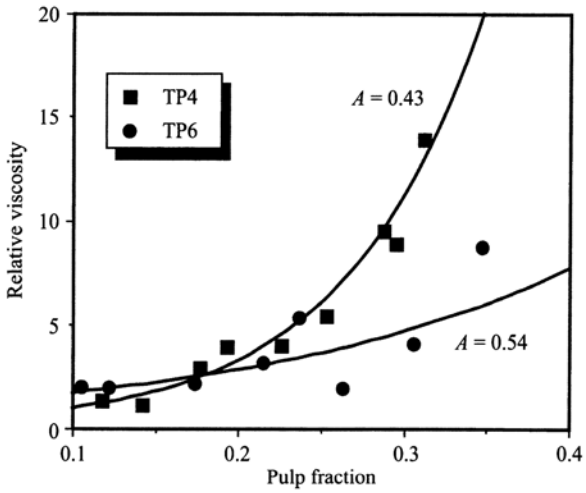

Fig. 2.7 Applicability of the model of Kitano et al. (1981) (Fig. 2.5) to tomato particles. (Yoo and Rao 1994)

They reported values of k in the range 2.50–3.82 for dispersions of rigid solids, and 1.70–1.85 for red blood suspensions. For gelatinized 2.6% tapioca STDs, the relative viscosity was calculated using Eq. 2.30:

$$\eta_{r_\infty} = \frac{\eta_\infty}{\eta_S} \tag{2.30}$$

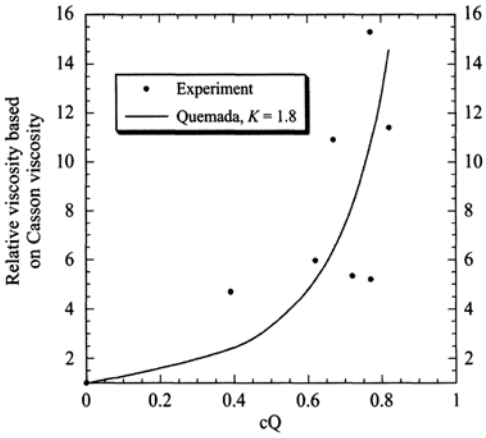

Fig. 2.8 The relative viscosity (η_r) values of tapioca starch dispersions strongly depended on their volume fraction. The line in the figure represents values predicted by the model of Quemada et al. (1985) with the structural parameter $k = 1.8$. (Tattiyakul et al. 2009)

where, $\eta_{r\infty}$ is the relative viscosity based on the Casson viscosity, η_∞ (mPa s) at 20 °C, and η_s 178 is the viscosity (mPa s) of the supernatant determined at 20 °C.

The model of Quemada et al. (1985) with the structural parameter $k = 1.80$ gave a satisfactory fit (Fig. 2.8). Because heated tapioca starch granules are deformable, the value $k = 1.80$ of red blood cells was selected for the data on tapioca STDs. Given that the Krieger–Dougherty (1959) model predictions were substantially different than experimental η_r values of starch dispersions (Ellis et al. 1989; Noel et al. 1993; Tattiyakul 1997), the reasonable applicability of Eq. 2.29 (Quemada et al. 1985) to tapioca STDs is noteworthy. However, the model of Quemada et al. (1985) is a phenomenological model, while that of Krieger–Dougherty (1959) is based on intrinsic viscosity of a single sphere. Saunders (1961) and Parkinson et al. (1970) found that the viscosity of a suspension increased with decrease in the average particle size. The particle size dependence can be explained by recognizing that as the particle size decreases, the number of particles in a given volume increases, resulting in a decrease in the mean distance between the particles. Another result of decreasing the particle size is to increase the potential for particle–particle interaction (Agarwala et al. 1992).

The important role of volume fraction on the structure of rigid sphere dispersions has been uncovered recently; as the volume fraction of hard spheres is increased, the equilibrium phase changes from a disordered fluid to coexistence with a crystalline phase ($0.494 < \phi < 0.545$), then to fully crystalline ($\phi = 0.545$), and finally to a glass ($\phi = 0.58$) (Pham et al. 2002).

Colloidal Glass

Studies using colloidal hard spheres (HS) have led to valuable insights in to their phase and rheological behavior: first, a disordered fluid to crystal transition at $\phi = 0.494$ and coexistence of crystal and liquid domains for $0.494 \leq \phi \leq 0.545$. Fur-

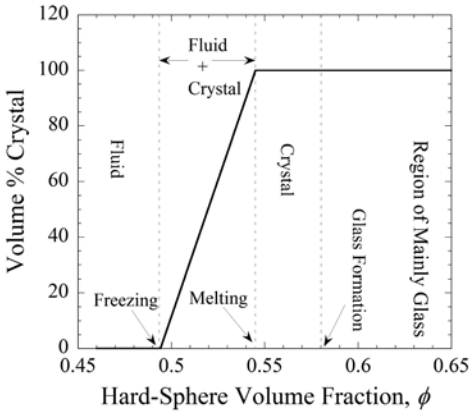

Fig. 2.9. Phase behavior of colloidal hard sphere dispersions, from Pusey and van Megen (1986)

ther, as the volume fraction of HS is increased, transition to fully crystalline state, and finally to a colloidal glassy state. (Pusey and van Megen 1986; Phan et al. 1996). The expression "colloidal glass" is used to differentiate it from the well- and long-known temperature-driven glassy state (Loveday et al. 2007).

The phase behavior of colloidal HS dispersions is summarized in Fig. 2.9 and it is discussed next. As the solids concentration is increased gradually, at a solids concentration, $\phi = 0.494$, crystals (clusters of particles) appear that coexist with the liquid. Thus, the coexistence of colloidal fluid and crystal phases is analogous to that of a simple liquid and solid at a first-order phase transition. Further, in the coexistence region: $0.494 \leq \phi \leq 0.545$, we find a linear dependence with ϕ which, when extrapolated to 0 and 100 %, provides the "freezing" and "melting" concentrations. The liquid to crystal transition at $\phi = 0.494$ is referred to as the beginning of freezing. These observations have been verified by others whose investigations were based on computer simulation, theory, and three-dimensional microscopy (e.g., Phan et al. 1996; Weeks et al. 2004).

As the volume fraction of solids, ϕ, is increased beyond $\phi = 0.545$, the particles are increasingly caged by others, and at a critical value, ϕ_G, the caging stops all long-range particle motion, and the system is considered to be glassy (Pham et al. 2002). Pusey and van Megen (1986) observed that the highly concentrated ($\phi > 0.58$), viscous, samples exhibited only partial heterogeneous crystallization even when left undisturbed for several months. The concentration of particles was sufficiently high that particle diffusion was hindered to the point where crystals did not form on that time scale and the suspensions remained in the metastable amorphous phase created by the earlier sample tumbling. Thus, for $\phi \approx 0.58$ hard-sphere colloidal dispersions form glasses and the glassy state is present over a range of solids concentration. The effective volume fraction of the most concentrated glassy sample was close to $\phi = 0.637$ expected for the random close-packed HS (so called Bernal) glass. The discovery of a glass composed of equal-sized spheres is especially interesting since, although there has been considerable theoretical work and computer simulations on such model glasses earlier, real glasses composed of spherical units were not identified experimentally.

Rheology of Protein Dispersions

Many protein particles are crystal shaped (Loveday et al. 2007). For example, bovine serum albumin (BSA) is a heart shaped globular protein molecule that can be approximated as an equilateral triangle with sides of 8 nm and a depth of 3 nm, and it has an equivalent hydrodynamic radius of 3.7 nm in the range of pH 4 and 8 (Ferrer et al. 2001). The β-lactoglobulin (β-LG) dimer is not spherical, but can be approximated as a prolate ellipsoid with length = 6.9 nm and width = 3.6 nm. From literature, it is known that the value of $\phi_{max} = \sim 0.71 - 0.74$ for prolate ellipsoid particles. In addition, in the Krieger-Dougherty model, one can use a value $[\eta] = 3.6$ for ellipsoid particles.

In milk, the casein is aggregated with calcium phosphate as casein micelles, with a mean size of about 300 nm. After the calcium phosphate is removed, the resulting sodium caseinate exists in solution mainly as a mixture of casein monomers and casein nanometer-scale particles (10–20 nm); further, gels may be produced from dispersions of sodium caseinate by heating, acidification, and high-pressure processing (Dickinson 2006). In sodium caseinate, different caseins interact with each other to form associated structures, which exist as a dynamic system of casein monomers, casein complexes, and aggregates (Lucey et al. 2000). The average radius of gyration of caseinate aggregates has been shown to be in the range 22–48 nm; the aggregates have been shown to be not spherical but highly elongated structures. The extent of aggregation of sodium caseinate depends on the relative proportions of the different monomeric caseins and also on the temperature, pH, ionic strength, and calcium ion concentration (Dickinson 2006).

Farrer and Lips (1999) obtained zero-shear viscosity data on dispersions of sodium caseinate (pH 6.8, 0.1 M NaCl) over the concentration range 3–28% w/v. Their values of relative viscosity were calculated using solvent viscosity of 1 mPa s. Panouille et al. (2005) obtained zero-shear viscosity data for dispersions of phosphocaseinate (pH 6.0, polyphosphate 2% w/v); the phosphocaseinate was obtained after the colloidal calcium phosphate had been removed from the casein micelles. An empirical model, based on concentration, C, (instead of volume fraction) was used to fit the relative viscosity data of the phosphocaseinate dispersions up to a concentration of about 10% w/v:

$$\eta_r = \left(1 - \frac{C}{C_c}\right)^{-2} \tag{2.31}$$

In Fig. 2.10, the relative viscosity data on sodium caseinate dispersions from different laboratories are shown. As expected, the viscosity increases gradually with concentration up to about 10% and then more steeply at higher concentrations. Pitkowski et al. (2008) noted that this behavior was also found in multiarm star polymers and polymeric micelles. The high-end sodium caseinate dispersions were of higher concentration than in previous studies (Farrer and Lips 1999; Panouille et al. 2005) and the viscosity data were in good agreement with the extrapolated data of Farrer and Lips (1999) (Loveday et al. 2010).

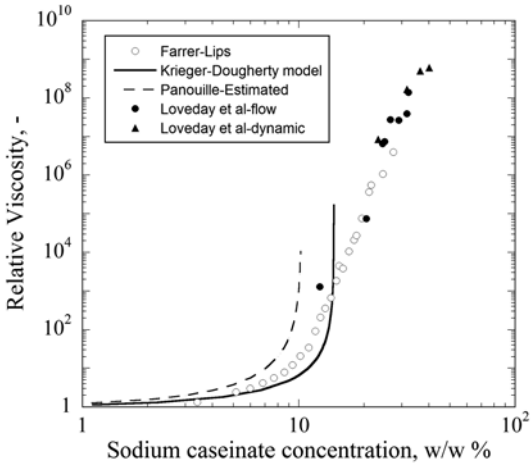

Fig. 2.10 Relative viscosity vs. concentration of Na caseinate dispersions. Data of Farrer-Lips (1999) on dispersions of Na caseinate pH = 6.8, 0.1 M NaCl (Loveday et al. 2010). Solid line: values using the Krieger and Dougherty (1959) model for hard spheres with $[\eta]=2.5$ and $\phi_{max}=0.65$. Dotted line: values calculated using equation that fit data on dispersions of phosphocaseinate (pH 6.0, polyphosphate 2% w/v) in water by Panouille et al. (2005)

The dashed line in Fig. 2.10 represents relative viscosity values of the phosphocaseinate dispersions predicted by the empirical model (Eq. 2–31). Also shown in this figure as a solid line are values of relative viscosity predicted by the Krieger-Dougherty model (Eq. 2–26) with $[\eta]=2.5$ and $\phi_{max}=0.65$. It is interesting to note that the values predicted by the model were lower than the experimental data up to a concentration of about 14% w/w, but increased more steeply than the data at higher concentrations. Because of uncertainties in the determination of the sodium caseinate particle volume fraction, the polydispersity of the particles, and their softness, the Krieger-Dougherty rheological model developed for hard-sphere dispersions predicted the trends accurately but not the absolute values of viscosity.

Modulus of Gels of Fractal Floes

In addition to the volume fraction of solids, their fractal nature also affects rheological properties. Shih et al. (1990) developed a scaling relationship for the elastic properties of colloidal gels by considering the structure of the gel network to be a collection of close packed fractal floes of colloidal particles. They defined two separate rheological regimes depending on the strength of the interfloc links relative to that of the floes themselves: (1) the strong-link regime is observed at low particle concentrations, allowing the floes to grow to be very large, so that they can be considered weak springs. Therefore, the links between floes have a higher elastic constant than the floes themselves, and (2) the weak-link regime is observed at high particle concentrations, where the small floes are stronger springs, and the links between floes have a lower elastic constant than the floes themselves. The weak-link regime should be applicable to gels that are well above the gelation threshold (Shih et al. 1990) where the elastic modulus, G', is related to the particle volume fraction (ϕ) by the following relationship:

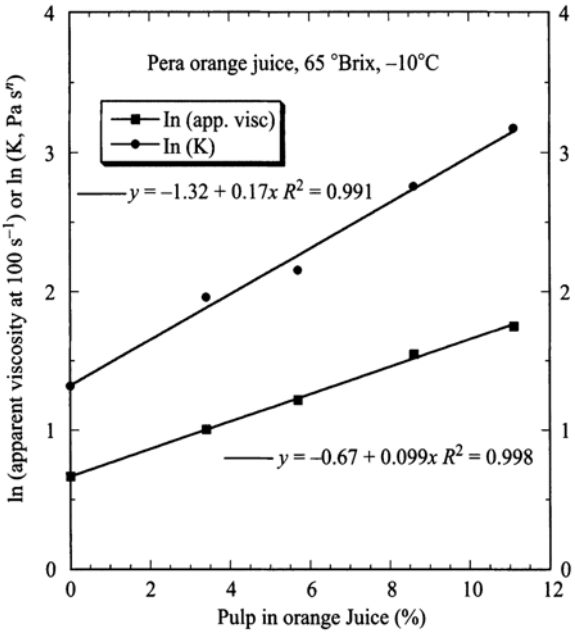

Fig. 2.11 Plateau modulus of starch dispersion plotted against volume fraction of starch granules. Fractal dimensions of the starch granules were calculated from the slopes of the lines

Table 2.3 Fractal dimension of selected foods based on rheological data. (Rao 2007)

Network of Particles	Fractal Dimension, D_f
Palm oil or lard fat	2.82–2.88
Cocoa butter	2.37
Salatrim®	2.90
Milk fat and/canola oil blends	1.97–1.99
Whey protein isolate + $CaCI_2$ gels	2.30–2.60
Soy protein isolate gels, pH 3.8 and 0.2 M NaCI	2.30
Starch gels	2.79–2.81
Egg white protein gel, pH 3.7	1.90–2.10

$$G' \sim \phi^{(d-2)/(d-D_f)} \tag{2.32}$$

where, D_f is the fractal dimension of the colloidal floe and d is the Euclidean dimension of the network—usually three. The power relationship between the modulus and the volume fraction of solids implied in Eq. 2.31 is illustrated in Fig. 2.11 for two gelatinized starch dispersions (Genovese and Rao 2003). Such plots have been utilized to determine the fractal dimension of several food gels (Table 2.3) and values of D_f between about 1.9 and 2.9 have been reported (Rao 2007). Wu and Morbidelli (2001) extended the above model to include gels that are intermediate between the strong-link and the weak-link regimes.

Effect of Soluble and Insoluble Solids Concentration on Apparent Viscosity of Foods

The effect of concentration on the zero-shear viscosity of biopolymer dispersions can be expressed in terms of the coil overlap parameter, $c[\eta]$, and the zero-shear specific viscosity as described in Chap. 4 in connection with food gum dispersions.

Unlike biopolymer dispersions where the intrinsic viscosity is known and the polymer concentration can be chosen a priori, often for fluid foods the concentration of soluble (e.g., pectins in fruit juices) and insoluble solids can be determined only posteriori, and the determination of their zero-shear viscosities is also difficult due to instrument limitation and due to the existence of yield stress. However, in many foods, it may be possible to identify the components, called key components, that play an important role in the rheological properties.

The effect of concentration (c) of soluble or insoluble solids on either apparent viscosity (η_a) or the consistency index of the power law model (K) can be described by either exponential or power law relationships:

$$\eta_a \propto \exp(ac) \tag{2.33}$$

$$\eta_a \propto c^b \tag{2.34}$$

$$K \propto \exp(a'c) \tag{2.35}$$

$$K \propto c^{b'} \tag{2.36}$$

where, a, a', b, and b′ are constants to be determined from experimental data. Other models that are applicable to specific foods are discussed under the flow properties of specific foods in Chaps. 4 and 5.

We consider the viscosity data on Pera concentrated orange juice (COJ) of Vitali (Vitali and Rao 1984a, b) to illustrate the exponential model for the effect of soluble solids (°Brix) and insoluble solids (% Pulp) (Tables 2.3 and 2.4). The influence of soluble solids on apparent viscosity at a shear rate of 100 s^{-1} (η_a, 100) and on K shown in Fig. 2.12 and that of insoluble solids on the same rheological parameters shown in Fig. 2.13 can be described by exponential relationships.

Table 2.4 Effect of °Brix on apparent viscosity and consistency index of the power law model, Pera orange juice, 5.7% pulp, −10 °C. (Vitali and Rao 1984a, b)

°Brix	($\eta_{a,100}$ Pa s	ln, $\eta_{a,100}$	K, Pa s^n	*ln* K
50.8	0.29	−1.2379	0.89	−0.1165
56.5	0.65	−0.4308	2.18	0.7793
57.9	0.83	−0.1863	2.56	0.9400
61.6	1.62	0.4824	5.61	1.7246
65.3	3.38	1.2179	23.58	3.1604

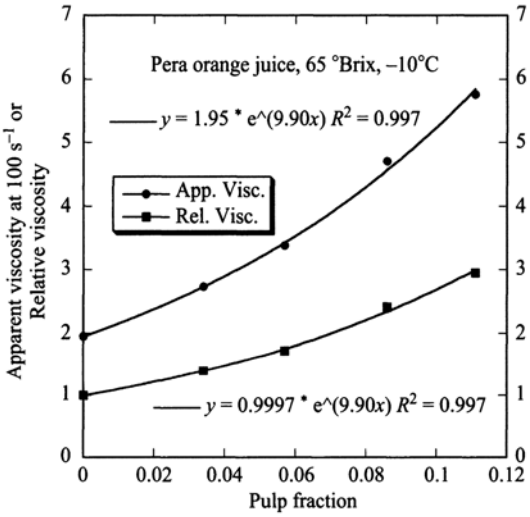

Fig. 2.12 The influence of insoluble solids on apparent viscosity at a shear rate of 100 s^{-1}(η_a, 100) and on the consistency coefficient, *K*, of pera concentrated orange juice, data of Vitali and Rao (1984b)

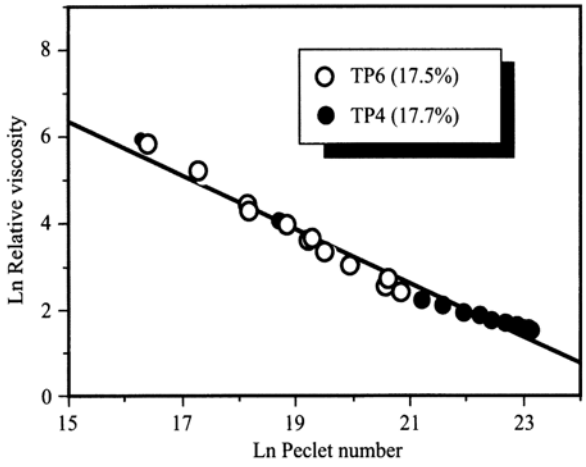

Fig. 2.13 The influence of soluble solids on apparent viscosity at a shear rate of 100 s^{-1} (η_a, 100) and on the consistency coefficient, *K*, of Pera concentrated orange juice, Data of Vitali and Rao (1984a)

The effect of concentration (*c*) of soluble solids (°Brix) and insoluble solids (Pulp) on either apparent viscosity or the consistency index of the power law model of FCOJ can be described by exponential relationships (Vitali and Rao 1984a, b). Equations 2.36 and 2.37 are applicable to the consistency coefficient (*K*) of the power law model. In the case of FCO J, it should be noted that insoluble solids are expressed in terms of pulp content determined on a 12 °Brix sample by centrifugation at 360 × g for 10 min (Table 2.5).

$$K = K^{c} \exp(B_K^{c}\ ^{o}\text{Brix}) \tag{2.37}$$

$$K = K^{p} \exp(B_K^{P}\ ^{o}\text{Brix}) \tag{2.37}$$

Table 2.5 Effect of Pulp content on apparent viscosity and consistency index of the power law model, pera orange juice, 65 °Brix − 10 °C. (Vitali and Rao 1984a, b)

Pulp %	$\eta_{a,\ 100}$ Pa s	$ln, \eta_{a,\ 100}$	K, Pa s^n	*ln* K
0	1.95	0.6678	3.74	1.3191
3.4	2.73	1.0043	7.11	1.9615
5.7	3.38	1.2179	8.63	2.1552
8.6	4.70	1.5476	15.77	2.7581
11.1	5.76	1.7509	23.91	3.1743

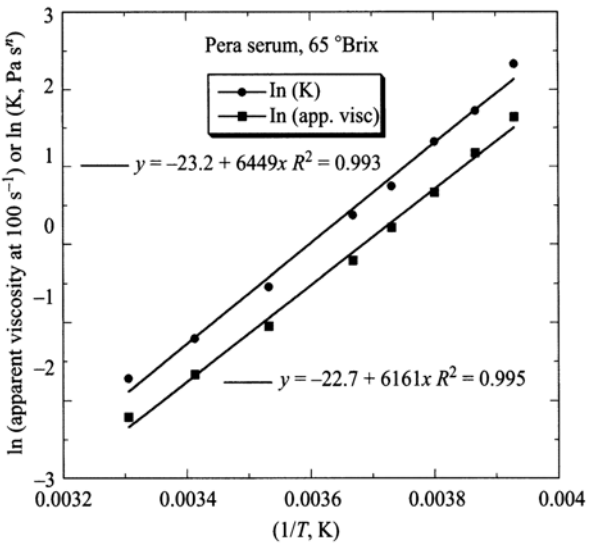

Fig. 2.14 The strong influence of pulp fraction on the viscosity of concentrated orange juice (COJ) and the relative viscosity (η_r) of COJ

where, K^c, K^p, B_K^C and B_K^P are constants.

The role of insoluble solids can be also studied in terms of the relative viscosity (η_r = apparent viscosity of COJ/apparent viscosity of serum) and pulp fraction (Fig. 2.12) and, as expected, such a plot has the limiting value of 1.0 at zero pulp fraction (serum). The curve in Fig. 2.14 illustrates the strong influence of pulp fraction on the viscosity of COJ. The values of η_a,100 also, as expected, follow a profile similar to that of η_r (Fig. 2.14). The two curves are described by the equations:

$$\eta_r = \exp(9.90 \times \text{pulp fraction}) \tag{2.39}$$

$$\eta_{a\ 100} = 1{,}95 \times \exp(9.90 \times \text{pulp fraction}) \tag{2.40}$$

Peclet Number of Dispersions

Yoo and Rao (1996) studied the influence of two different sizes of tomato pulp particles (TP4 and TP6) at a pulp weight fraction of 17 % in terms of Peclet number and

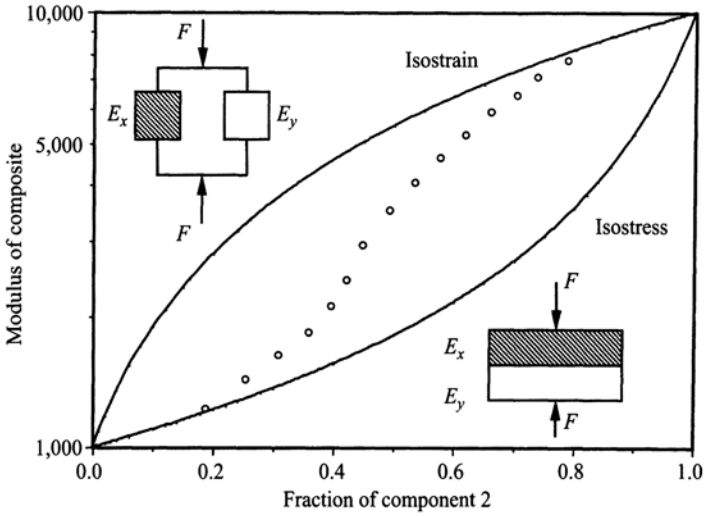

Fig. 2.15 Peclet number versus relative viscosity of tomato pulp particles. At equal values of pulp weight fraction, a TP6 sample with small diameter particles was more viscous than a TP4 sample with large diameter particles

relative viscosity (Krieger 1985; Tsai and Zammouri 1988). The Peclet numbers (P_e) were calculated using the equation:

$$P_e = \frac{\eta_o r_o^3 \dot{\gamma}}{kT} \tag{2.41}$$

where, η_0 is the viscosity of the suspending liquid (serum), r_0 is the particle radius, k is the Boltzmann constant (1.38×10^{-23} N m K^{-1}), and T is the absolute temperature.

The Peclet number compares the effect of imposed shear with the effect of diffusion of the particles. When $P_e >> 1$, hydrodynamic effects dominate and a dispersion of spherical particles exhibits shear-thinning behavior. In contrast, when $P_e << 1$, the distribution of particles is only slightly altered by the flow (Hiemenz and Rajagopalan 1997). As shown in Fig. 2.15, at equal values of pulp weight fraction, a TP6 sample with small diameter particles was more viscous than a TP4 sample with large diameter particles. A nearly linear relationship exists between the relative viscosity of TP sample and the Peclet number. Similar linear relationship was found for glass bead suspensions (Tsai and Zammouri 1988). However, the slope of the linear relationship of TP6 sample is slightly higher than that of TP4 sample, indicating that at high-shear rates, the TP6 aggregates with small particles are more sensitive to shear than those with large particles. The different aspect ratios of the TP4 and TP6 particles discussed above is another reason for the deviation from a single linear relationship. From these observations, it can be concluded that the effect of

particle size on the relative viscosity of tomato puree sample can be correlated with the Peclet number of the particle.

Emulsions

Many foods are oil-in-water or water-in-oil emulsions (o/w), with dispersed particle size range of 0.01 – 10 μm. Many of the equations discussed for food suspensions are also applicable to emulsions. In a dilute emulsion, the particles are far apart and the interparticle interactions are relatively weak. Skim milk is an example of a dilute emulsion with the concentration of fat droplets (dispersed phase) < 1 %. However, in a concentrated emulsion, the particles are close to each other and there are strong interparticle interactions. Mayonnaise has a dispersed phase (oil) concentration of 70 – 80 %. As with foods containing insoluble solids, the volume fraction of the dispersed phase in emulsions is important.

The separation of phases in an emulsion occurs spontaneously in the direction of decreasing Gibbs free energy. Thus it can be said that there is more surface energy in an emulsion when the dispersed droplets are in a highly subdivided state than when they are in a coarser state of subdivision. To be stable, an o/w emulsion should exhibit yield stress, and the forces applied to the continuous phase by the dispersed phase due to the applicable forces (e.g., gravity and buoyancy) should be below the emulsion's yield stress.

The words stable and unstable are often used to describe emulsions that are better understood by examining the underlying processes. The coarsening of a thermodynamically unstable emulsion is called coalescence or aggregation; coalescence is a process by which two or more particles fuse together to form a single larger particle; aggregation is a process by which small particles lump together to form aggregates (Hiemenz and Rajagopalan 1997). The van der Waals force between particles in a dispersion is usually attractive and is strong at short distances between particles. Therefore, the emulsion will be unstable and coagulate unless there are repulsive interactions between particles. Two methods are used to overcome van der Waals attraction: (1) electrostatic stability in which the electrostatic force resulting from overlapping electrical double layers of two particles, and (2) polymer-induced or steric stability in which a suitable polymer that is adsorbed on the particle surfaces may be used. In food emulsions, polymer-induced stability is encountered commonly.

Very often, the microstructure and the macroscopic states of dispersions are determined by kinetic and thermodynamic considerations. While thermodynamics dictates what the equilibrium state will be, kinetics determine how fast that equilibrium state will be determined. While in thermodynamics the initial and final states must be determined, in kinetics the path and any energy barriers are important. The electrostatic and the electrical double-layer (the two charged portions of an interfacial region) play important roles in food emulsion stability. The Derjaguin-Landau-

Verwey-Overbeek (DLVO) theory of colloidal stability has been used to examine the factors affecting colloidal stability.

An emulsifier may be thought of as a single chemical component or mixture of components that have the capacity to promote emulsion formation and stabilization by interfacial action; in contrast, a stabilizer confers long-term stability on an emulsion involving often adsorption or another mechanism. Polymers, such as gum Arabic, egg albumin, casein, and gelatin have been used for a long time to stabilize food emulsions. Other stabilizers include xanthan gum, guar gum, and whey protein isolate. Because some of these are charged polymers (polyelectrolytes), their stabilizing influence is due to both electrostatic and polymeric effects, that is, electrosteric stabilization. Lecithins (e.g., from egg yolk and soybean) are the most important food emulsifiers derived from natural sources without chemical reaction (Dickinson 1993). They consist of mixtures of many phospholipid components with phosphatidylcholine (PC) and phosphatidylethanolamine (PE) being present in large proportions.

A simplified view of some of the possible effects of polymer molecules on a dispersion include (Hiemenz and Rajagopal 1997): (1) at low polymer concentrations bridging flocculation, where a polymer chain forms bridges by adsorbing more than one particle, (2) at higher polymer concentrations, "brush-like" layers can form on the solid particles that can mask the influence of van der Waal's attraction between the particles, thereby imparting stability, called steric stabilization, (3) at moderate to high polymer concentrations, the polymer chains may be excluded in the region between the particles resulting in depletion flocculation, and (4) at high polymer concentrations, polymer-depleted regions may be created by demixing the polymer resulting in depletion stabilization. Generally, polymers containing only one kind of repeat unit (homopolymers) are not good for steric stabilization. One requirement is that the polymer be adsorbed at the oil–water interface and the polymer is considered to reside partially at surface sites and partially in loops or tails in the solution. Under the right circumstances, an adsorbed polymer layer stabilizes a dispersion against aggregation. It may be said that the approaching particles in an aggregation step experience an increase in free energy of repulsion, ΔG_R, that can be divided into enthalpic (ΔH_R) and entropie (Δ, S_R) contributions:

$$\Delta G_R = \Delta H_R - T\Delta S_R \tag{2.42}$$

In Eq. 2.39, the terms describe changes in enthalpy and entropy in the overlapping region of the adsorbed layers of two particles. Because ΔH_R and ΔS_R can be either positive or negative, it is possible for the value of ΔG_R to change sign with change in temperature and the critical temperature for the onset of flocculation is known as the critical flocculation temperature (Hiemenz and Rajagopalan 1997).

Because of the many factors affecting the rheology of food emulsions, the rheological properties cannot be predicted a priori so that experimental studies on model o/w and food emulsions are necessary. Whey proteins, especially β-lactoglobulin, possess good emulsification properties and whey protein stabilized emulsions can be convert-

ed into emulsion gels by thermal treatment (Aguilera and Kessler 1989; Dickinson and Yamamoto 1996a). In general, the incorporation of protein-coated emulsion droplets into a heat-set globular protein network resulted in an increase in gel strength. Further, a self-supporting heat-set emulsion gel can be was formed at a protein content much lower than that required under similar thermal processing conditions (Dickinson and Yamamoto 1996b). Addition of pure egg yolk L-α- phosphatidylcholine after emulsification caused an increase in strength of a heat-set β-lactoglobulin emulsion gels (Dickinson and Yamamoto 1996b). The positive influence of pure egg lecithin added after emulsification on the elastic modulus of the whey protein concentrate emulsion gel was attributed to lecithin-protein complexation. Crude egg lecithin also gave a broadly similar increase in gel strength. However, pure soybean lecithin was not as effective in reinforcing the network and crude soybean lecithin was ineffective (Dickinson and Yamamoto 1996a). These results support the general hypothesis that filler particles (e.g., globular protein-coated droplets) that interact with a gel matrix (a network of aggregated denatured whey protein) tend to reinforce the network and increase the gel strength (Dickinson and Yamamoto 1996b).

Other relevant studies on physical properties of emulsions are those of McClements et al. (1993), Dickinson and Pawlowsky (1996), Dickinson et al. (1996), and Demetriades et al. (1997). The application of nuclear magnetic resonance (NMR) technique (Simoneau et al. 1993) and ultrasonic spectroscopy (Demetriades et al. 1996) to study the stability of emulsions were discussed. The rheological behavior of salad dressings and mayonnaises that are emulsions will be discussed in Chap. 5.

Effect of Temperature on Viscosity

A wide range of temperatures are encountered during processing and storage of fluid foods, so that the effect of temperature on rheological properties needs to be documented. The effect of temperature on either apparent viscosity at a specified shear rate (Eq. 2.42) or the consistency index, K, of the power law model (Eq. 2.43) of a fluid can be described often by the Arrhenius relationship. The effect of temperature on apparent viscosity can be described by the Arrhenius relationship:

$$\eta_a = \eta_{\infty A} \exp(E_a/RT) \tag{2.43}$$

where, η_a is the apparent viscosity at a specific shear rate, $\eta_{\infty A}$ is the frequency factor, E_a is the activation energy (J mol^{-1}), R is the gas constant (J mol^{-1}K^{-1}), and T is temperature (K).

Although the name of Arrhenius is associated with Eq. 2.42, Moore (1972) credited J. de Guzman Carrancio for first pointing out this relationship in 1913. The quantity E_a is the energy barrier that must be overcome before the elementary flow process can occur. The term: exp $(-E_a/RT)$ may be explained as a Boltzmann fac-

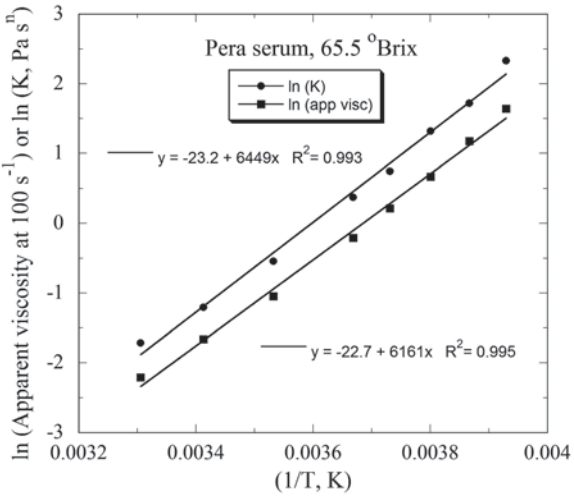

Fig. 2.16 Applicability of the Arrhenius Model to the apparent viscosity versus temperature data on a concentrated orange juice serum sample (Vitali and Rao 1984b) is Shown

tor that gives the fraction of the molecules having the requisite energy to surmount the barrier. Hence, E_a is the activation energy for viscous flow. From a plot of ln η_a (ordinate) versus ($1/T$) (abscissa), E_a equals (slope × R) and η_{∞_A} is exponential of the intercept.

The Arrhenius equation for the consistency coefficient is:

$$K = K_\infty \exp\left(E_{aK}/RT\right) \tag{2.44}$$

where, K_∞ is the frequency factor, E_{ak} is the activation energy (J/mol), R is the gas constant, and T is temperature (K). A plot of ln K (ordinate) versus ($1/T$) (abscissa) results in a straight line, and E_{ak} = (slope × R), and K_∞. is exponential of the intercept. The activation energy should be expressed in joules (J), but in the earlier literature it has been expressed in calories (1 calorie = 4.1868 J). The applicability of the Arrhenius model to the apparent viscosity versus temperature data on a concentrated orange juice serum sample (Vitali and Rao 1984a, b) is shown in Fig. 2.16.

The Arrhenius equation did not describe very well the influence of temperature on viscosity data of concentrated apple and grape juices in the range 60–68 °Brix (Rao et al. 1984, 1986). From nonlinear regression analysis, it was determined that the empirical Fulcher equation (see Ferry 1980, p. 289, Soesanto and Williams 1981) described the viscosity versus temperature data on those juice samples better than the Arrhenius model (Rao et al. 1986):

$$\log \eta = A' + \frac{B'}{T - T_\infty} \tag{2.45}$$

Table 2.6 Magnitudes of the parameters of the Arrhenius Equation for the effect of temperature on concentrated Apple and Grape juices. (Rao et al. 1986)

Sample	η_∞	E_a, $kJ\ mol^{-1}$	SSQ	R^2
Apple 68.3 °Brix	1.366E-15	79	0.10260	1.00
Apple 64.9 °Brix	1.671E-15	76	0.02870	1.00
Apple 60.1 °Brix	2.610E-13	62	0.00110	1.00
Apple 55.0 °Brix	5.050E-11	48	0.00100	0.99
Grape 68.3 °Brix	2.150E-14	73	0.31770	1.00
Grape 64.5 °Brix	9.810E-13	63	0.03950	1.00
Grape 59.9 °Brix	2.940E-12	58	0.00620	1.00
Grape 54.0 °Brix	7.610E-11	49	0.00130	1.00

Table 2.7 Magnitudes of the parameters of the Fulcher Equation for the effect of temperature on concentrated Apple and Grape juices. (Rao et al. 1986)

Sample	A′	B′	T_∞	SSQ	R^2
Apple 68.3 °Brix	−7.26	1,049	132.8	0.01356	1.00
Apple 64.9 °Brix	−7.56	1,035	130.9	0.01360	1.00
Apple 60.1 °Brix	−6.87	911	124.3	0.00208	1.00
Apple 55.0 °Brix	−6.07	896	94.0	0.00048	1.00
Grape 68.3 °Brix	−6.75	1,039	125.7	0.14110	1.00
Grape 64.5 °Brix	−6.65	1,041	115.1	0.02150	1.00
Grape 59.9 °Brix	−6.81	1,048	107.0	0.00080	1.00
Grape 54.0 °Brix	−6.56	1,085	84.5	0.00080	1.00

The magnitudes of the parameters of the Arrhenius and the Fulcher equations for the studied concentrated apple and grape juices are given in Tables 2.6 and 2.7, respectively. The physical interpretation of the three constants in the Fulcher equation is ambiguous, but by translating them in terms of the WLF parameters their significance can be clarified and it is functionally equivalent to the WLF equation (Ferry 1980; Soesanto and Williams 1981):

$$\log\left(\frac{\eta}{\rho T}\Big/\frac{\eta_0}{\rho_0 T_0}\right)=-\frac{c_1^0\left(T-T_0\right)}{c_2^0+\left(T-T_0\right)} \tag{2.46}$$

Specifically, T_∞ and B' are related to c_1^0, c_2^0 and a reference temperature T_0, often called the glass transition temperature, by the following two equations:

$$T_\infty = T_0 - c_2^0 \tag{2.47}$$

$$B' = \frac{c_1^0}{\left(T_0 - T_\infty\right)} \tag{2.48}$$

However, it should be pointed out that Soesanto and Williams (1981) also determined the values of the glass transition temperature of the very high concentration sugar solutions (91.9–97.6% by weight) by regression techniques and not experimentally.

The WLF equation was also used to correlate viscosity versus temperature data on honeys (Al-Malah et al. 2001; Sopade et al. 2003). Because of the empirical nature of the Fulcher equation and the empirical origin of the WLF equation, their use with viscosity data of relatively dilute fruit juices serves mainly the objective of obtaining a useful correlation.

Combined Effect of Concentration and Temperature

The flow behavior index (n) is assumed to be relatively constant with temperature and concentration, and the combined effects of temperature and concentration on the power law consistency index, K, are described by:

$$K = Ac^{b1} \exp(E_a/RT) \tag{2.49}$$

Tomato concentrates and concentrated milk samples are examples of foods in this category. Alternatively, the combined effects of temperature and concentration on the power law consistency index, K, are described by:

$$K = A' \exp\left(\frac{E_a}{RT} + bc\right) \tag{2.50}$$

Mixing Rules for two Component Blends

Earlier, the role of suspended particles in fluid media in increasing the viscosity of a suspension and different equations relating the volume fraction of solids were discussed. For general two component or polymer composites, the Takayanagi models (Ross-Murphy 1984; Sperling 1986) provide means for calculating the upper (so called isostrain) and lower (so called isostress) limits of values for the shear modulus G_c of a composite formed from components x and y with shear moduli G_x and G_y, respectively. In the former, the polymers are arranged in parallel with respect to deformation, while in the latter they are arranged in series. In the parallel arrangement, the deformation of the weaker component is limited by the modulus of the stronger material and both components are deformed to the same extent (isostrain). In the series arrangement, the strength of the weaker component limits the force transmitted to the stronger material; therefore, both are subjected to the same stress (isostress).

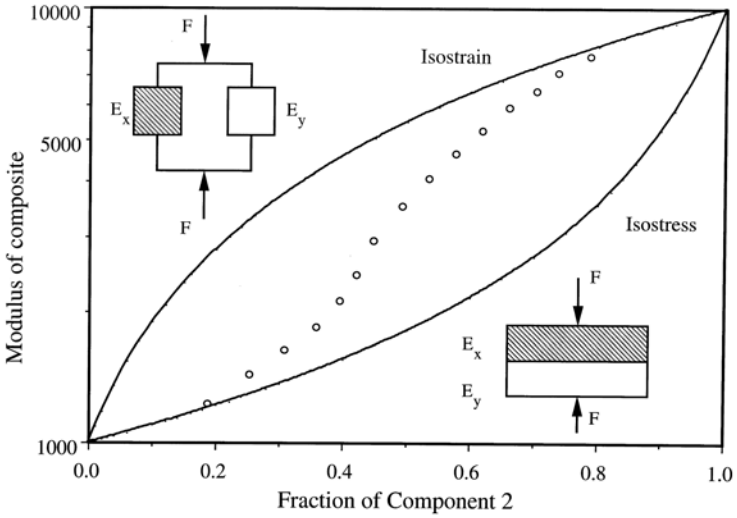

Fig. 2.17 Modulus of the composite gel (G_c) Plotted against volume fraction of component y (G=10,000). When the weaker component (x, G=1,000 Pa) dominates and becomes the continuous phase, G_c follows the lower bound isostress limit, with increasing fraction of y, there will be a phase inversion and G_c reaches the upper bound limit, path indicated by open circles

If ϕ_x and $\phi_y = 1 - \phi_x$ are the respective volume fractions of the two components, the equations for the upper and lower bound values are:

$$G_c = \phi_x G_x + \phi_y G_y \quad \text{(upper bound, isostrain)} \tag{2.51}$$

$$\left(1/G_c\right) = \left(\phi_x/G_x\right) + \left(\phi_y/G_y\right) \quad \text{(lower bound, isostress)} \tag{2.52}$$

Values of G_c predicted by the above two models are shown in Fig. 2.17. Implicit in the above models is that the experimental value of G_c lies between those of G_x and G_y. For a simple phase-separated system, the lower bound form (isostress) should predict G_c prior to phase inversion when the supporting phase (x) is the weaker one. It will then show a transition to the upper bound behavior. More complex models can be found in Sperling (1986).

The Takayanagi models have been used to better understand the rheological behavior of a starch-soyprotein system (Chap. 4), tomato paste (Chap. 5), and mixed gel systems (Chap. 6). However, given that most foods contain several major components ($\tilde{c}$), the number and distribution of phases (P) is much more complex as seen from the phase rule:

$$\mathrm{P} = (\tilde{c} - \tilde{f} + 2) \tag{2.53}$$

where, $\tilde{f}$ is the number of degrees of freedom.

Treatment of Rheological Data Using Models

Prior to using a model for description of rheological data, it would be desirable tocritically examine a number of issues, such as:

1. How reliable are the data? Are the data reproducible? Are the measurement techniques reliable? Are the test samples reproducible, reliable, and suitable for rheological measurements?
2. Plot the data (σ—$\dot{\gamma}$)-look for trends in data and artifacts of rheometer. Sometimes, most, but not all, of the data can be used for subsequent analysis. If the data are not reliable, why fit models?
3. Rheological model: (a) Is it appropriate for the experimental data? (b) How reliable is the model parameter estimation software? Has the reliability of the software been checked? (c) What are you looking for in the data (e.g., effect of temp.)? (d) Compare experimental data with a model's predictions because R^2 values often do not indicate the appropriateness of the model for the selected data!

References

Abdel-Khalik, S. I., Hassager, O., and Bird, R. B. 1974. Prediction of melt elasticity from viscosity data. *Polymer Eng. and Sci*. 14: 859–867.

Agarwala, M. K., Patterson, B. R., and Clark, P. E. 1992. Rheological behavior of powder injection molding model slurries. *J. Rheol*. 36: 319–334.

Aguilera, J. M. and Kessler, H. G. 1989. Properties of mixed and filled dairy gels. *J. Food Sei*. 54: 1213–1217, 1221.

Al-Malah, K.-I.-M., Abu-Jdayil, B., Zaitoun, S., and Al-Majeed-Ghzawi, A. 2001. Application of WLF and Arrhenius kinetics to rheology of selected dark-colored honey. *J. Food Process Eng*. 24(5): 341–357.

Barnes, H. A. and Walters, K. 1989. The yield stress myth? *Rheol. Acta* 24: 323–326.

Barnes, H. A., Hutton, J. F., and Walters, K. 1989. An Introduction to Rheology, Elsevier Science Publishers B.V., Amsterdam, The Netherlands.

Bird, R. B., Dai, G. C., and Yarusso, B. J. 1982. The rheology and flow of viscoplastic materials. *Rev. Chem. Eng*. 1: 1–70.

Brodkey, R. S. 1967. The Phenomena of Fluid Motions, Addison-Wesley, Reading, MA.

Casson, N. 1959. A flow equation for pigment-oil suspensions of the printing ink type, in Rheology of Disperse Systems, ed. C. C. Mill, pp. 82–104, Pergamon Press, New York.

Choi, G. R. and Krieger, I. M. 1986. Rheological studies on sterically stabilized model dispersions of uniform colloidal spheres II. Steady-shear viscosity. *J. Colloid Interface Sei*. 113: 101–113.

Cross, M. M. 1965. Rheology of non-Newtonian fluids: a new flow equation for pseudoplastic systems. *J. Colloid Sci*. 20: 417–437.

Da Silva, P. M. S., Oliveira, J. C., and Rao, M. A. 1997. The effect of granule size distribution on the rheological behavior of heated modified and unmodified maize starch dispersions. *J. Texture Stud*. 28: 123–138.

Demetriades, K., Coupland, J., and McClements, D. J. 1996. Investigation of emulsion stability using ultrasonic spectroscopy, in 1996 IFT Annual Meeting Book of Abstracts, pp. 109–110, Institute of Food Technologists, Chicago, IL.

Demetriades, K., Coupland, J., and McClements, D. J. 1997. Physical properties of whey protein stabilized emulsions as related to pH and NaCI. *J. Food Sei*. 62: 342–347.

Dervisoglu, M. and Kokini, J. L. 1986. Steady shear rheology and fluid mechanics of four semi-solid foods. *J. Food Sei*. 51: 541–546, 625.

Dickinson, E. 1993. Towards more natural emulsifiers. Trends Food *Sei*. Technol. 4: 330–334.

Dickinson, E. 2006. Structure formation in casein-based gels, foams, and emulsions. *Colloids Surf A* 288:3–11.

Dickinson, E. and Pawlowsky, K. 1996. Effect of high-pressure treatment of protein on the rheology of flocculated emulsions containing protein and polysaccharide. *J. Agric. Food Chem*. 44: 2992–3000.

Dickinson, E. and Yamamoto, Y. 1996a. Viscoelastic properties of heat-set whey protein-stabilized emulsion gels with added lecithin. *J. Food Sei*. 61:811–816.

Dickinson, E. and Yamamoto, Y. 1996b. Effect of lecithin on the viscoelastic properties of *β*-lactoglobulin-stabilized emulsion gels. *Food Hydrocollids* 10: 301–307.

Dickinson, E., Hong, S.-T., and Yamamoto, Y. 1996. Rheology of heat-set emulsion gels containing beta-lactoglobulin and small-molecule surfactants. *Neth. Milk Dairy J*. 50: 199–207.

Einstein, A. 1906. Eine neue bestimmung der molekuldimension. *Ann. Physik* 19: 289–306.

Einstein, A. 1911. Berichtigung zu meiner arbeit: Eine neue bestimmung der molekuldimension. *Ann. Physik* 34: 591–592.

Ellis, H. S., Ring, S. G., and Whittam, M. A. 1989. A comparison of the viscous behavior of wheat and maize starch pastes. *J. Cereal Sei*. 10: 33–44.

Fang, T. N., Tiu, C., Wu, X., and Dong, S. 1996. Rheological behaviour of cocoa dispersions. *J. Texture Stud*. 26: 203–215.

Fang, T., Zhang, H., Hsieh, T. T., and Tiu, C. 1997. Rheological behavior of cocoa dispersions with cocoa butter replacers. *J. Texture Stud*. 27: 11–26.

Farrer, D. and Lips, A. 1999. On the self-assembly of sodium caseinate. *Int Dairy J* 9:281–6.

Ferrer, M. L., Duchowicz, R., Carrasco, B., Torre, J. G., Acuña, A. U. 2001. The conformation of serum albumin in solution: A combined phosphorescence depolarization-hydrodynamic modeling study. *Biophysical Journal* 80:2422–2430.

Ferry, J. D. 1980. Viscoelastic Properties of Polymers, John Wiley, New York.

Genovese, D. B. and Rao, M. A. 2003. Role of starch granule characteristics (volume fraction, rigidity, and fractal dimension) on rheology of starch dispersions with and without amylose. *Cereal Chem*. 80: 350–355.

Giboreau, A., Cuvelier, G., and Launay, B. 1994. Rheological behavior of three biopolymer/water systems with emphasis on yield stress and viscoelastic properties. *J. Texture Stud*. 25: 119–137.

Hiemenz, R C. and Rjagopalan, R. 1997. Principles of Colloid and Surface Chemistry, 3rd ed., Marcel Dekker, Inc., New York.

Holdsworth, S. D. 1971. Applicability of rheological models to the interpretation of flow and processing behavior of fluid food products. *J. Texture Stud*. 4: 393–418.

Holdsworth, S. D. 1993. Rheological models used for the prediction of the flow properties of food products: a literature review. *Trans. Inst. Chem. Engineers* 71, Part C: 139–179.

Jacon, S. A., Rao, M. A., Cooley, H. J., and Walter, R. H. 1993. The isolation and characterization of a water extract of konjac flour gum. *Carbohydr. Polym*. 20: 35–41.

Jinescu, V. V. 1974. The rheology of suspensions. *Int. Chem. Eng*. 143: 397–420.

Kimball, L. B. and Kertesz, Z. I. 1952. Practical determination of size distribution of suspended particles in macerated tomato products. *Food Technol*. 6: 68–71.

Kitano, T., Kataoka, T., and Shirota, T. 1981. An empirical equation of the relative viscosity of polymer melts filled with various inorganic fillers. *Rheol. Acta* 20: 207–209.

Krieger, I. J. 1985. Rheology of polymer colloids, in Polymer Colloids, eds. R. Buscall, T. Corner, and J. F. Stageman, pp. 219–246, Elsevier Applied Science, New York.

Krieger, I. M. and Dougherty, T. J. 1959. A mechanism for non-Newtonian flow in suspensions of rigid spheres. *Trans. Soc. Rheol*. 3: 137–152.

Launay, B., Doublier, J. L., and Cuvelier, G. 1986. Flow properties of aqueous solutions and dispersions of polysaccharides, in Functional Properties of Food Macromolecules, eds. J. R. Mitchell and D. A. Ledward, pp. 1–78, Elsevier Applied Science Publishers, London.

Lopes da Silva, J. A. L., Gonpalves, M. P., and Rao, M. A. 1992. Rheological properties of high-methoxyl pectin and locust bean gum solutions in steady shear. *J. Food Sei*. 57: 443–448.

Loveday, S. M., Creamer, L. K., Singh, H. and Rao, M. A. 2007. Phase and rheological behavior of high-concentration colloidal hard-sphere and protein dispersions. *J Food Sci*. 72(7): R101–107.

Loveday, S. M., Rao, M. A., Creamer, L. K. and Singh, H. 2010. Rheological behavior of high-concentration sodium caseinate dispersions. *J Food Sci*. 74:N30–N35.

Lucey, J. A., Srinivasan, M., Singh, H. and Munro, P. A. 2000. Characterisation of commercial and experimental sodium caseinates by multi-angle laser light scattering and size-exclusion chromatography. *J Agric Food Chem* 48:1610–6.

McClements, D. J., Monaham, F. J., and Kinsella, J. E. 1993. Effect of emulsion droplets on the rheology of whey protein isolate gels. *J. Texture Stud*. 24: 411–422.

Metz, B., Kossen, N. W. F., and van Suijdam, J. C. 1979. The rheology of mould suspensions, in Advances in Biochemical Engineering, eds. T. K. Ghose, A. Fiechter and N. Blakebrough, Vol. 2, p. 103, Springer Verlag, New York.

Metzner, A. B. 1985. Rheology of suspensions in polymeric liquids. *J. Rheol*. 29: 739–775.

Mizrahi, S. and Berk, Z. 1972. Flow behaviour of concentrated orange juice: mathematical treatment. *J. Texture Stud*. 3: 69–79.

Moore, W. J. 1972. Physical Chemistry, 4th ed., Prentice Hall, Inc., Englewood Cliffs, New Jersey.

Noel, T. R., Ring, S. G., and Whittam, M. A. 1993. Physical properties of starch products: structure and function, in Food Colloids and Polymers: Stability and Mechanical Properties, eds. E. Dickinson and P. Wolstra, pp. 126–137. Royal Soc. Chem., Cambridge, UK.

Ofoli, R. Y., Morgan, R. G., and Steffe, J. F. 1987. A generalized rheological model for inelastic fluid foods. *J. Texture Stud*. 18: 213–230.

Panouille, M., Benyahia, L., Durand, D. and Nicolai, T. 2005. Dynamic mechanical properties of suspensions of micellar casein particles. *J Colloid Interface Sci* 287:468–75.

Paredes, M. D. C., Rao, M. A., and Bourne, M. C. 1988. Rheological characterization of salad dressings. 1. Steady shear, thixotropy and effect of temperature. *J. Texture Stud*. 19: 247–258.

Parkinson, C., Matsumoto, S., and Sherman, P. 1970. The influence of particle-size distribution on the apparent viscosity of non-Newtonian dispersed system. *J. Colloid Interface Sei*. 33: 150–160.

Pham, K. N., Puertas, A. M., Bergenholtz, J., Egelhaaf, S. U., Moussaid, A., Pusey, P. N., Schofield, A. B., and Cates, M. E. 2002. Multiple glassy states in a simple model system. *Science* 296: 104–106.

Phan, S-E., Russel, W. B., Cheng, Z., Zhu, J., Chaikin, P. M., Dunsmuir, J. H. and Ottewill, R. H. 1996. Phase transition, equation of state, and limiting shear viscosities of hard sphere dispersions. *Physical Review E* 54:6633–6645.

Pitkowski, A., Durand, D. and Nicolai, T. 2008. Structure and dynamical properties of suspensions of sodium caseinate. *J. Colloid Interface Sci*. 326:96–102.

Poslinski, A. J., Ryan, M. E., Gupta, R. K., Seshadri, S. G., and Frechette, F. J. 1988. Rheological behavior of filled polymeric systems I. Yield stress and shear-thinning effects. *J. Rheol*. 32: 703–735.

Pusey, P. N, and van Megen, W. 1986. Phase behaviour of concentrated suspensions of nearly hard colloidal spheres. *Nature* 320:340–342.

Quemada, D., Fland, P., and Jezequel, P. H. 1985. Rheological properties and flow of concentrated diperse media. *Chem. Eng. Comm*. 32:61–83.

Rao, M. A. 2007. Influence of food microstructure on food rheology, in Understanding And Controlling the Microstructure of Complex Foods, ed. D. J. McClements, Woodhead Publishing Ltd., Cambridge, UK.

Rao, M. A. and Cooley, H. J. 1983. Applicability of flow models with yield for tomato concentrates. *J. Food Process Eng*. 6:159–173.

Rao, M. A., Cooley, H. J., and Vitali, A. A. 1984. Flow properties of concentrated fruit juices at low temperatures. *Food Technology* 38(3): 113–119.

Rao, M. A., Shallenberger, R. S., and Cooley, H. J. 1986. Effect of temperature on viscosity of fluid foods with high sugar content, in Engineering and Food, eds. M. LeMaguer and P. Jelen, Vol. 1, pp. 23–31, Elsevier Applied Science Publishers, New York.

Rayment, P., Ross-Murphy, S. B., and Ellis, P. R. 1998. Rheological properties of guar galactomannan and rice starch mixtures. II. Creep measurements. *Carbohydr. Polym*. 35: 55–63.

Ross-Murphy, S.B. 1984. Rheological methods. In Biophysical Methods In Food Research, pp. 138–199, ed. H.W. Chan, Blackwell Scientific Publications, London.

Saunders, F. L. 1961. Rheological properties of monodisperse latex systems I. Concentration dependence of relative viscosity. *J. Colloid Sei*. 16: 13–22.

Servais, C., Ranc, H., and Roberts, I. D. 2004. Determination of chocolate viscosity. *J. Texture Stud*. 34(5–6): 467–498.

Shih, W.-H., Shih, W. Y., Kim, S.-I., Liu, J., and Aksay, I. A. 1990. Scaling behavior of the elastic properties of colloidal gels. *Phys. Rev*. A 42(8): 4772–4779.

Simoneau, C., McCarthy, M. J., and German, J. B. 1993. Magnetic resonance imaging and spectroscopy for food systems. *Food Res. Intern*. 26: 387–398.

Soesanto, T. and Williams, M. C. 1981. Volumetric interpretation of viscosity for concentrated and dilute sugar solutions. *J. Phys. Chem*. 85: 3338–3341.

Sopade, P.-A., Halley, P., Bhandari, B., D'Arcy, B., Doebler, C., and Caffin, N. 2003. Application of the Williams-Landel-Ferry model to the viscosity-temperature relationship of Australian honeys. *J. Food Eng*. 56(1): 67–75.

Sperling, L. H. 1986. Introduction to Physical Polymer Science, John Wiley, New York.

Steiner, E. H. 1958. A new rheological relationship to express the flow properties of melted chocolate. Rev. *Internationale de la Choeolatiere*. 13: 290–295.

Tattiyakul, J. 1997. Studies on granule growth kinetics and characteristics of tapioca starch dispersion during gelatinization using particle size analysis and rheological methods. M. S. thesis, Cornell University, Ithaca, NY.

Tattiyakul, J., Liao, H-J. and Rao, M.A. 2009. Role of structure in the measurement of flow properties of food and starch dispersions: a review. *International Journal of Food Properties* 12(1):2–10.

Tiu, C. and Boger, D. V. 1974. Complete rheological characterization of time-dependent food products. *J. Texture Stud*. 5: 329–338.

Tiu, C., Podolsak, A. K., Fang, T. N., and Watkins, J. B. 1992. Rheological behavior of water-creosote and creosote-water emulsions. *Rheol. Acta* 31: 381–389.

Tsai, S. C. and Zammouri, K. 1988. Role of interparticular van der Waals force in rheology of concentrated suspensions. *J. Rheol*. 32: 737–750.

Vitali, A. A. and Rao, M. A. 1984a. Flow properties of low-pulp concentrated orange juice: effect of temperature and concentration. *J. Food Sei*. 49: 882–888.

Vitali, A. A. and Rao, M. A. 1984b. Flow properties of low-pulp concentrated orange juice: Serum viscosity and effect of pulp content. *J. Food Sei*. 49: 876–881.

Vocadlo, J. J. and Moo Young, M. 1969. Rheological properties of some commercially available fats. *Can. Inst. Food Technol. J*. 2: 137–140.

Weltman, R.N. 1943. Breakdown of thixotropic structure as a function of time. *J. Appl. Phys*. 14: 343–350.

Wildemuth, C. R. and Williams, M. C. 1984. Viscosity of suspensions modeled with a shear-dependent maximum packing fraction. *Rheol. Acta* 23: 627–635.

Wu, H. and Morbidelli, M. 2001. A model relating structure of colloidal gels to their elastic properties. *LangmuirM*: 1030–1036.

Yoo, B. and Rao, M. A. 1994. Effect of unimodal particle size and pulp content on rheological properties of tomato puree. *J. Texture Stud*. 25: 421–436.

Yoo, B. and Rao, M. A. 1996. Creep and dynamic rheological behavior of tomato concentrates: effect of concentration and finisher screen size. *J. Texture Stud*. 27: 451–459.

Yoo, B., Rao, M. A., and Steffe, J. F. 1995. Yield stress of food suspensions with the vane method at controlled shear rate and shear stress. *J. Texture Stud*. 26: 1–10.